New critical behavior in Einstein-Yang-Mills collapse

Matthew W. Choptuik*
Center for Relativity, The University of Texas at Austin, Austin, Texas 78712-1081
and Institute for Theoretical Physics, University of California, Santa Barbara, California 93106-4030

Eric W. Hirschmann†
Southampton College, Long Island University, Southampton, New York 11968

Robert L. Marsa‡
Reliant Data Systems, 13915 Burnet Road, Suite 200, Austin, Texas 78728
(Received 23 April 1999; published 23 November 1999)

We extend the investigation of the gravitational collapse of a spherically symmetric Yang-Mills field in Einstein gravity and show that, within the black hole regime, a new kind of critical behavior arises which separates black holes formed via type I collapse from black holes formed through type II collapse. Further, we provide evidence that these new attracting critical solutions are in fact the previously discovered colored black holes with a single unstable mode. [S0556-2821(99)03024-6]

PACS number(s): 04.25.Dm, 04.40.−b, 04.70.Bw

I. INTRODUCTION

It is by now relatively well known that gravitational collapse can produce rich structure even within highly simplified systems such as spherical symmetry. In particular, near the threshold of black hole formation, the strong field dynamics of general relativity exhibits critical phenomena.

The pioneering work demonstrating this critical behavior in the collapse of a single massless scalar field [1] has been supplemented by investigations of gravitational waves [2], a perfect fluid [3] and a variety of other matter models, all of which exhibit the same general characteristics. Indeed, to our knowledge no system which has been studied in this context has been shown *not* to exhibit this critical phenomena.

At this point in the subject's development, dynamical evolutions (solutions of the full partial differential equations of motion), in tandem with analytic and perturbative calculations have given us a reasonable understanding of many of the phenomenological details of critical behavior in collapse. (See [4] for an excellent review of the subject.)

In light of this, one of the more interesting discoveries in some of the more recently studied models [5–9] is the presence of two distinct types of behavior at the threshold of black hole formation. Specifically, in these models, certain regions of parameter space (initial-data space) are found to yield near-critical collapsing configurations which display self-similarity and, in the super-critical regime, a scaling law which is continuous in the black hole mass. By analogy with the theory of phase transitions, this is called a type II transition. However, it is found that other regions of parameter space lead to critical collapse which has a static (or periodic) solution as an intermediate attractor—this results in a black hole transition with a nonzero mass gap. Again, in analogy with the discontinuous behavior in order parameter which frequently accompanies first order phase transitions, this is called type I behavior. For the case of the Einstein-Yang-Mills (EYM) model studied in [5], the static solution appearing in type I collapse is the well-known $n=1$ Bartnik-Mckinnon solution [10], while for the massive scalar model considered in [6], the type I threshold solutions are apparently unstable members of the family of ''oscillating soliton stars'' which have previously been constructed by Seidel and Suen [11], albeit in a different context. Finally, in the case of Einstein-Skyrme (ES) collapse considered in [7,8], a static type I solution was observed, which, as in the EYM case, had previously been constructed and studied within a purely static *ansatz* [12]. As noted above, each of these three models also exhibits type II behavior—in the case of massive scalar collapse [6], the type II critical solution is the same one originally observed in massless scalar collapse [1], and, interestingly, in the ES model, the type II solution is evidently identical [9] to that observed in the EYM model [5]. Heuristically, one expects type II behavior in *any* collapse model where the initial configuration can be made sufficiently ''kinetic-energy-dominated'' (ultra-relativistic), whereas type I behavior is expected only in those models which have an intrinsic length scale (or equivalently, mass scale), and which have some type of self-interaction which can ''balance'' the attractive gravitational interaction.

As noted in the concluding remarks of [5], hints of further interesting phenomenology in the EYM model have been seen in the super-critical regime where all evolutions are characterized by black hole formation. In this paper we study this regime in more detail and present evidence for a new type of critical transition in which the intermediate attractors are the ''minimally unstable'' (one unstable mode in perturbation theory) colored black holes discovered by Bizon [13], and independently by Volkov and Gal'tsov [14]. This result is, of course, analogous to the discovery that the $n=1$ Bartnik-Mckinnon solution is the intermediate attractor for

*Electronic address: matt@einstein.ph.utexas.edu
†Electronic address: ehirsch@bach.liu.edu
‡Electronic address: marsa@einstein.ph.utexas.edu

type I collapse. Crucially, in order to accurately model the dynamics of super-critical solutions for long times after the formation of an event horizon, we use black-hole excision techniques. Such methods were first successfully employed in a dynamical context by Seidel and Suen [15], and have subsequently been studied and implemented by many other authors (see [16] and references therein for a more extensive discussion). However, to our knowledge, this is the first time that excision has been used to study critical collapse, and we feel our results highlight the power and potential of the strategy to elucidate issues relating to the formation and long-time evolution of black holes. Our adoption of excising techniques necessitates the use of a different coordinate system than that used in [5]—that work used polar slicing and areal spatial coordinates, a system which generalizes the usual Schwarzschild coordinates to time-dependent spacetimes. As is well-known, the $t=$ constant slices in the polar or areal system cannot penetrate apparent horizons—thus, for all practical purposes, the slices remain outside of event horizons and therefore cannot be used in conjunction with excision. We therefore retain areal spatial coordinates, but adopt maximal slicing—in this case the slices *do* cross apparent and event horizons, and excision techniques *can* be used.

The outline of the remainder of the paper is as follows. The next section describes the EYM model and the equations of motion we subsequently solve numerically. We pay particular attention to gauge and coordinate choices, as well as to regularity, boundary and initial conditions for the fields. In Sec. III we describe our numerical scheme, focusing on our specific coordinate choices and on some details of our black-hole excising technique. In Secs. IV and V we describe our results and conclusions.

II. EQUATIONS AND ASSUMPTIONS

We are interested in investigating the gravitational collapse of a self-gravitating Yang-Mills gauge field. To begin, let us consider the action for an EYM theory:

$$S=\int d^4x\sqrt{-g}\left[\frac{R}{16\pi G}-\frac{1}{g^2}F^a_{\mu\nu}F^{a\mu\nu}\right] \tag{1}$$

where $F^a_{\mu\nu}$ is the Yang-Mills field strength tensor. On varying the action with respect to the metric, $g_{\mu\nu}$, and the gauge connection, A^a_μ, we get the general equations of motion. We simplify these further by making some additional assumptions. In particular, we choose the gauge group to be $SU(2)$ and focus on spherically symmetric gravitational collapse. This places restrictions on both the spacetime metric and the form of the gauge connection. Even so, the equations we derive have a rather general form as can be seen in Eqs. (A6)–(A22). Subsets of these equations have been considered in a variety of different contexts. In particular [5] evolved a version of the Einstein-Yang-Mills equations in polar ($K^\theta_\theta=0$), areal ($b=1$) coordinates with the additional assumption on the Yang-Mills field that the connection A^a_μ was purely magnetic.

Since our interest here is to consider the same model studied in [5], but to penetrate into the super-critical regime of the phase space, we will likewise make the ''magnetic *ansatz*.'' As described in the Appendix, together with appropriate gauge choices, this *ansatz* effectively sets all but one of the components of the gauge connection to zero.

In addition to making these gauge choices we must also choose a coordinate system. As mentioned in the Introduction, in order to evolve the system for long times to the future of black hole formation, we choose maximal time slices and areal (or radial) spatial coordinates.

As detailed in the Appendix, the equations can now be written in the following form. The evolution equations are

$$\dot{\Pi}=\left[\beta\Pi+\frac{\alpha}{a}\Phi\right]'+\frac{\alpha a}{r^2}w(1-w^2) \tag{2}$$

$$\dot{\Phi}=\left[\frac{\alpha}{a}\Pi+\beta\Phi\right]' \tag{3}$$

$$\dot{w}=\frac{\alpha}{a}\Pi+\beta w' \tag{4}$$

and the constraint equations are

$$w'=\Phi \tag{5}$$

$$\alpha''=\alpha'\left(\frac{a'}{a}-\frac{2}{r}\right)+\frac{2\alpha}{r^2}\left(a^2-1+\frac{2ra'}{a}\right)+4\pi G\alpha(S-3\rho) \tag{6}$$

$$a'=a\frac{1-a^2}{2r}+\frac{3}{2}ra^3K^{\theta 2}_\theta+4\pi Gra\rho \tag{7}$$

$$K^{\theta\prime}_\theta=-\frac{3}{r}K_\theta{}^\theta+4\pi G\left(\frac{\Pi\Phi}{g^2ar^2}\right) \tag{8}$$

where the matter stress-energy terms are given by

$$S-3\rho=\frac{a^2(1-w^2)^2}{2g^2r^4}+\frac{1}{g^2r^2}(\Phi^2+\Pi^2) \tag{9}$$

$$\rho=\frac{a^2(1-w^2)^2}{4g^2r^4}+\frac{1}{2g^2r^2}(\Phi^2+\Pi^2). \tag{10}$$

We also note that we have an algebraic relation for the sole component, β, of the shift vector, $\beta^i=(\beta,0,0)$:

$$\beta=\alpha rK^\theta_\theta. \tag{11}$$

In addition to the equations of motion, we need boundary conditions on the fields. These are determined by demanding regularity at the origin of spherical symmetry, and by enforcing an outgoing condition on the radiation fields at large radius. This latter condition assumes that there is no radiation coming in from outside our finite mesh. This is not completely true, as in general there will be backscattering of the propagating fields off regions of high curvature. However, if our domain of integration is large enough, the contributions from this scattering are dynamically negligible.

The demand for a regular origin results in boundary conditions on the fields at $r=0$. From Eqs. (6) and (7) it can be seen that $\alpha'(t,0)=a'(t,0)=0$, as well as $a(t,0)=1$. In addition, $\beta(t,0)=K^{\theta}_{\theta}(t,0)=0$. For the matter fields, $w(t,0)=\pm 1$ and $w'(t,0)=0$, so that the auxiliary variables Π and Φ are both zero at the origin. We note that these conditions constrain the Yang-Mills field, w, to be in a vacuum state at $r=0$.

For initial data, we choose a time-symmetric kink for the gauge potential which was previously used in [5]. This pulse is given by

$$w(0,r)=\left[1+a\left(1+\frac{br}{s}\right)e^{-2(r/s)^2}\right]\tanh\left(\frac{x-r}{s}\right) \tag{12}$$

$$\dot{w}(0,r)=0, \tag{13}$$

with the parameters a and b chosen such that $w(0,0)=1$ and $w'(0,0)=0$. The two parameters x and s define the center and width of the pulse, respectively. They also serve as the two parameters which we will vary in order to explore the phase space. We note that the implementation of this data in [5] was incorrect but ultimately had no effect on the overall conclusions of that work. We have fixed the implementation of the kink data here and note a minor improvement in the conservation of energy.

III. NUMERICAL APPROACH AND BLACK HOLE EXCISION

It should be emphasized that we do not incorporate any form of adaptive mesh refinement into our numerical approach. Instead, we use a fixed uniform grid with a mesh spacing which is sufficiently fine to uncover the new critical behavior. The drawback to this approach, of course, is that we are unable to fully resolve the discretely self-similar solutions which arise near the type II black hole threshold. However, our primary interest here is in the supercritical regime, and we are satisfied that previous work has established the nature of the type II transition.

What *is* important in this work is the use of black hole excision techniques which allow us to evolve well beyond the formation of the black hole. We discretize the evolution equations (2)–(4) using two time levels with centered time differences, and angled spatial differences as described in [16]. The constraint equations are then integrated outward from the origin. Equation (6), the slicing equation, is rewritten in first order form

$$\delta'=\delta\left(\frac{a'}{a}-\frac{2}{r}\right)+\frac{2\alpha}{r^2}\left(a^2-1+\frac{2ra'}{a}\right)+4\pi G\alpha(S-3\rho) \tag{14}$$

$$\alpha'=\delta. \tag{15}$$

The apparent horizon equation in maximal-areal coordinates is simply

$$arK^{\theta}_{\theta}=1. \tag{16}$$

Thus, we can compute a characteristic function C such that

$$C=\begin{cases}1 & \text{if } arK^{\theta}_{\theta}\leqslant\mu_H,\\ 0 & \text{if } arK^{\theta}_{\theta}>\mu_H,\end{cases}$$

where μ_H is a threshold value, ostensibly unity, but set to a slightly larger value in practice—typically, $\mu_H=1.1$—to ensure that the inner boundary lies strictly within the apparent horizon. At any time, the characteristic function tells us which grid points are deemed to be inside $[C(r,t)=0]$ or outside $[C(r,t)=1]$ the horizon. As the system evolves, we recompute C at each time step and simply ''discard'' any grid points for which $C=0$. The radial locations of these grid points will then generally satisfy $r\leqslant r_H(t)$, where $r_H(t)$ is the instantaneous inner boundary of the computational domain, and roughly coincides with the location of the apparent horizon. We need *no* boundary conditions for the functions evolved with equations (2)–(4) since the characteristic directions at $r=r_H$ are such that only events with $r\geqslant r_H$ are in the past domain of dependence. We can therefore use the discrete form of the evolution equations up to *and including* the inner boundary point. However, the constraint equations (6)–(8) must have an inner boundary condition. Until a horizon is formed, we can simply use conditions derived from regularity. Once a horizon forms, however, we need an alternative. If the horizon initially forms at time $t=T$ and radial coordinate $r=R$, then for a function $f\in\{a,K^{\theta}_{\theta}\}$, we use $f(R,T)$ as the initial boundary value for f. We then evolve f along this boundary using the evolution equation for f. The evolution equations that we use are as follows:

$$\dot{a}=\beta\left[4\pi ra^3\rho+\frac{a}{2r}(1-a^2)+\frac{3}{2}ra^3K^{\theta 2}_{\theta}\right]+raK^{\theta}_{\theta}\delta-4\pi ra\alpha j_r, \tag{17}$$

$$\dot{K}^{\theta}_{\theta}=3K^{\theta}_{\theta}\left(\frac{1}{2}\alpha K^{\theta}_{\theta}-\frac{\beta}{r}\right)+4\pi(\alpha S^r_r-\beta j_r)+\frac{\alpha}{2r^2a^2}(a^2-1)-\frac{\delta}{ra^2}. \tag{18}$$

Since the lapse α does not have an evolution equation, we simply leave α and δ ''frozen'' at whatever specific values they have when excision at that particular radius, $r_H(t)$, begins.

Finally, we note that the programs which we used to generate the results that we will describe below were written in RNPL (Rapid Numerical Prototyping Language) [17]. This language has been specifically designed to facilitate the differencing and subsequent numerical solution of partial differential equations.

IV. RESULTS

On evolution of the equations, we verify previously examined aspects of this system as discussed in [5]. In particular, we find that in different regions of the parameter space, there are both types of critical behavior at the threshold of

black hole formation. We observe type I behavior, wherein black holes turn on at finite mass and the intermediate attractor is the $n=1$ Bartnik-Mckinnon solution. We also confirm aspects of type II collapse in the appropriate region of parameter space. This includes such things as echoing and the scaling relation for the black hole mass. However, because our code does not employ mesh-refinement, we are unable to fully reproduce the results of [5]. However, as discussed previously, our main emphasis here is to address the outstanding question of what happens in the super-critical region and to the future of black hole formation.

On evolving into the supercritical (black hole) regime, we find that the dynamics of the resulting spacetimes exhibit two distinct types of behavior which we describe below. It turns out that these can be characterized by the asymptotic vacuum state of the Yang-Mills potential w. These two behaviors are related to the type I and type II critical collapses identified previously.

The original type I collapse is described, in part, by a black hole which forms with finite mass. Slightly supercritical type I evolutions, now continued well to the future of black hole formation confirm this behavior, as one would expect. In addition, after the black hole is formed, part of the remaining Yang-Mills field outside the horizon radiates to infinity and some of it falls down the black hole causing the black hole to grow. How much larger the initial black hole becomes through the infall of additional matter depends, in part, on where in the parameter space the evolution begins. Eventually, however, and in accordance with what might be expected from the no-hair theorems, the exterior spacetime settles down to a Schwarzschild black hole with the Yang-Mills field in its vacuum state. In general, for slightly supercritical collapse (either type I or type II), as the remaining mass-energy radiates away the gauge potential approaches one of its two vacuum values: $w=\pm 1$. For the case of slightly super-critical type I collapse, in the asymptotic regime, the gauge potential always picks the $w=-1$ vacuum state [recall that our initial data family (12) has $w(t,0)=+1$ and $w(t,\infty)=-1$]. This turns out to be true even for collapsing configurations which are no longer just slightly super-critical but are, in fact, well into the black hole regime. We can thus characterize a sort of ''generalized'' supercritical type I collapse by the asymptotic value of the gauge potential w.

When type II collapse is considered, the overall picture is broadly the same. Again, after the original black hole forms (at *finite* mass since we are slightly super-critical) some of the matter remaining in the region exterior to the black hole falls into the black hole causing it to grow and the rest is radiated off to infinity. The resulting exterior spacetime again settles down to Schwarzschild with the Yang-Mills field in its vacuum state. However, the gauge potential in the slightly super-critical type II collapse approaches its other vacuum value: $w\rightarrow +1$. Similarly, further into the type II super-critical regime (where we should emphasize the discretely self-similar nature of the critical solution is no longer clear and where the black holes which form all have finite mass) we find ''generalized'' super-critical type II collapse which can be characterized by an asymptotic value of the gauge potential of $w=+1$.

It is worth commenting here that our terminology has become a bit loose. We have been speaking of type I and type II collapse well into the super-critical regime when in fact these terms originally referred to types of critical behavior in a very small neighborhood of the exact critical solutions. For instance, as one moves away from the type II threshold, the discrete self-similarity of the exactly critical solution is no longer clearly exhibited by configurations which collapse to a black hole. In addition, a significant fraction of the mass present will end up in the black hole. This is to be contrasted with the tiny black holes that can be formed in near-critical type II collapse. It should also be made clear that type I and type II do not refer to different *types* of black holes. The end-state exterior geometry in all of these evolutions is a Schwarzschild black hole. However, we are, in a sense, generalizing the concepts of type I and type II collapse to distinguish two kinds of collapse *dynamics* in the super-critical regime.

It quickly becomes clear that these regions are well defined in parameter space and it becomes natural to try and find the boundary separating them. Indeed, the problem reduces to tuning a single parameter across the threshold between these two types of collapse dynamics. What we find is that at the threshold between these two types of dynamics a static solution emerges as the intermediate attractor for this new near-critical collapse. The type II side of this threshold exhibits the following near-critical evolution. As the field collapses, a finite mass black hole is formed. The remaining field exterior to the black hole then approaches a static, nontrivial configuration. After some time the field then departs from the static configuration and disperses to infinity leaving the original black hole virtually unchanged. The gauge potential in this case approaches the vacuum value of $w=+1$ and thus this side of the threshold is part of the generalized type II collapse dynamics. The type I side of this threshold has, of course, a very similar development initially. Again, a black hole of finite mass is formed exactly as before and is followed by the approach of the exterior Yang-Mills field to the static solution. However, as the field leaves the static solution, most of the matter collapses into the black hole with only a small portion radiating off to infinity. The gauge potential, in this case, approaches the vacuum state of $w=-1$. Figures 1 and 2 show the development of these two cases overlayed with the static, intermediate attractor which is the exactly critical solution.

Since we are in the super-critical regime, these new, exactly critical solutions are themselves black holes with Yang-Mills hair. Indeed, these attractors are the colored black holes discovered by Bizon and independently by Volkov and Galtsov [13,14] shortly after the discovery of the Bartnik-Mckinnon solutions. In general, these colored, static black hole solutions are described by their horizon radius (or, relatedly, their mass) r_h and the number n of zero crossings of the Yang-Mills potential w. The solutions which serve here as intermediate attractors in the dynamical collapse are the lowest lying colored black holes with $n=1$. Subsequent to their discovery, it was shown that these black holes are un-

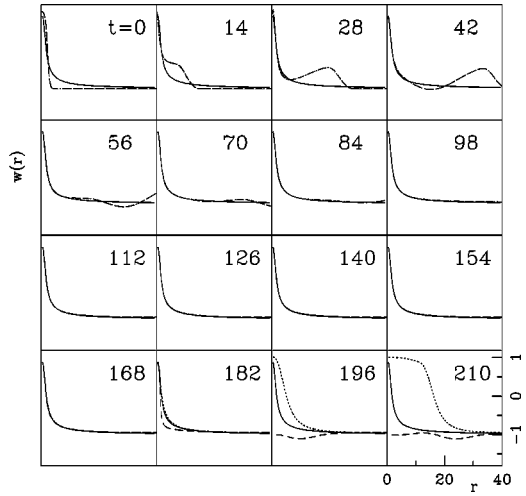

FIG. 1. Time sequences of the Yang-Mills potential w for both sub- and super-critical evolutions, overlayed with a static, colored black hole solution. Both evolutions are calculated to machine precision, i.e., $|p-p^*|/p^* \lesssim 10^{-15}$. The solid line is the static solution, the dashed line is the generalized type I solution, where part of the Yang-Mills field of the colored black hole collapses to a second, larger black hole, and the dotted line is the generalized type II solution, in which the remaining Yang-Mills field surrounding the colored black hole disperses to infinity. The calculations shown here use the kink data defined in Eq. (12). We fix the center of the pulse to be $x=2.16$, and perform our parameter search on s $(=p)$, the width of the pulse. These plots use the original radial coordinate, r. The initial colored black hole that forms has a radius of $r \approx 0.55$ on a domain from $r=0$ to $r=40$; a fixed uniform radial grid with 3201 points is used for all calculations. In the generalized type I case, the second and larger black hole forms with a radius of $r \approx 1.69$. Note that after the black hole forms, we do not plot points at locations within the horizon radius. This illustrates that our horizon excision continues the evolution only outside the black hole. As can be seen, the agreement between the static solution and the intermediate attractor to which the dynamical solutions temporarily evolve is excellent. The static solution is obtained by solving the static equations [ordinary differential equations (ODEs)] for a colored black hole of radius $r=0.55$.

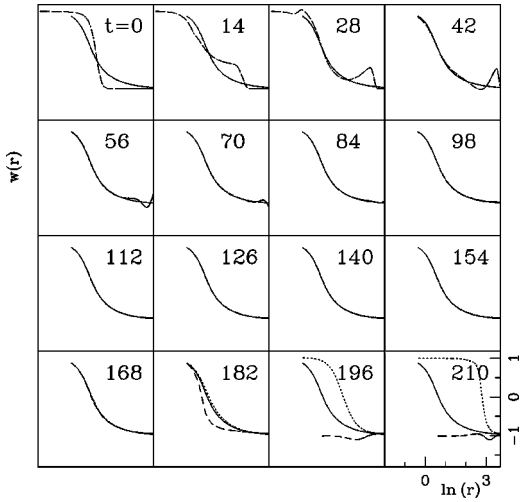

FIG. 2. Time sequence of the Yang-Mills potential as shown in Fig. 1—here the wave forms are plotted using a logarithmic radial coordinate.

stable. In particular, the colored black holes with label n have $2n$ unstable modes [18–20]. Of these $2n$ unstable modes, n arise from spherically symmetric perturbations in the gravitational sector away from staticity and another n unstable modes arise from perturbations in the sphaleron sector, i.e., away from the magnetic *ansatz* for the Yang-Mills fields. Since we are solving the nonlinear evolution equations while remaining within the magnetic *ansatz* we would expect our data to excite all the unstable modes within the gravitational sector while exciting none of the unstable modes in the sphaleron sector. As a result, we would expect the $n=1$ family of solutions to have a single unstable mode, thus making it relevant to critical collapse. The picture of this new critical solution in the black hole regime having a single unstable mode thus accords perfectly with previous understanding of both type I and type II collapse.

This new critical behavior within the black hole regime is, in many ways, qualitatively similar to that of the type I collapse. Solutions in one of these new interpolating families asymptote to one of the static, colored black hole solutions, $Y_1(r;r_h)$. Initial data for collapsing configurations close to one of the critical solutions will approach $Y_1(r;r_h)$, and remain in its vicinity for some amount of time T, as measured, for example, by an observer at infinity. The evolution will then peel off the static solution with the remaining field either dispersing to infinity or collapsing and adding a finite amount of mass to the already present black hole. One can quantify the amount of time spent near the static solution in the same way as with the type I collapse. The time, as measured by an asymptotic observer, is $T \approx -\lambda \ln|p-p^*|$, where the coefficient λ is the characteristic time scale for the collapse of the unstable solution $Y_1(r;r_h)$ or, in other words, the inverse Lyapounov exponent of the single unstable mode.

With our evolutions, we confirm this relation and can calculate the value of λ in the manner described in [5]. For Figs. 1 and 2, where the static solution has a black hole radius of $r_h \approx 0.55$, we confirm the linear relation and find $\lambda \approx 4.88$ as shown in Fig. 3.

Once we have established the existence of these new, colored critical solutions, it then becomes straightforward to map out parameter space for our choice of initial data. Figure 4 does this for the main region of interest. Figure 5 is a schematic drawing of the mass of the black hole as a function of the two initial data parameters.

Figure 4 should be compared to Fig. 1 in [5]. There, it was suggested that there was a coexistence between black holes exhibiting both types of critical behavior. However, that suggestion was based on evolutions which did not actually continue to the future of the resulting black hole. Thus, up to this point, only the region marked ''dispersion'' had been well explored. Evolutions had been performed in the black hole regime, but detailed understanding of what happened in collapse was largely limited to times prior to the formation of the black hole. Now, with our use of apparent horizon boundary conditions, we can explore more completely this super-critical region. Thus, what is actually

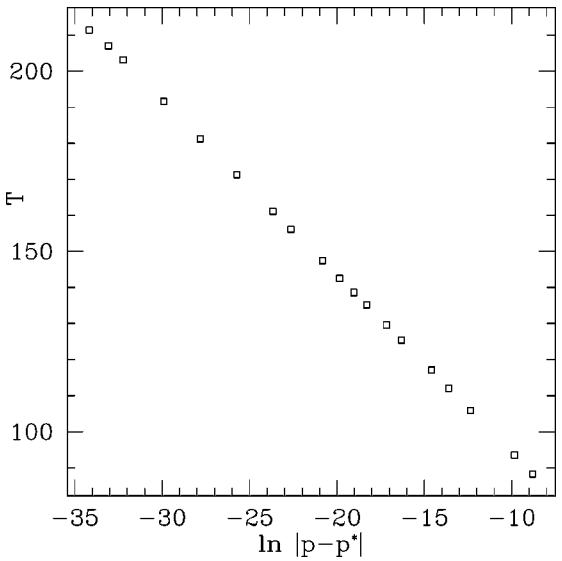

FIG. 3. Plot of the elapsed time (as measured by an observer at infinity) in generalized type II collapse before the zero of the w field crosses $r=35$. As the exactly critical solution is approached in parameter space, i.e., $p\rightarrow p^*$, the dynamical fields spend more time on the critical solution; specifically, the lifetime of the static configuration is $T\approx-\lambda\ln|p-p^*|$. Since the early part of the dynamics is unchanged as $p\rightarrow p^\star$, the total time before the lingering field escapes and passes a finite radial value depends only on $|p-p^*|$. Thus we can estimate λ by measuring this total time as a function of $\ln|p-p^*|$. A straightforward least squares fit of this data yields $\lambda\approx4.88$.

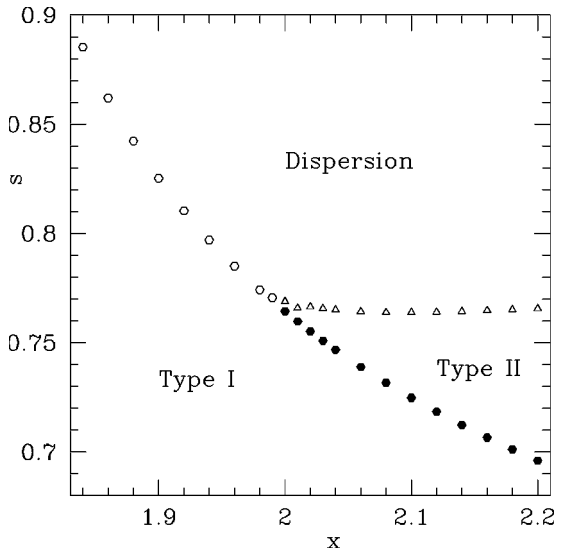

FIG. 4. Plot of the phase space for the two parameter family of kink data given by (12). Each point represents a critical solution at a level of $|p-p^*|/p^*\lesssim10^{-4}$ and sits on one of the thresholds separating two of the three phases. The open hexagons represent type I critical solutions which separate configurations that disperse from those that form a finite size black hole. We confirm that the intermediate attractor in this case is the $n=1$ Bartnik-Mckinnon solution, as found in [5]. The open triangles represent type II critical solutions which separate configurations that disperse from those that form an infinitesimal black hole. The filled hexagons represent the new black hole critical solutions separating the generalized type I and type II collapse dynamics as described in the text. These critical solutions are the $n=1$ colored black holes. They are parametrized by their horizon radius, such that as the ''triple point'' is approached along the critical line, the radius of the black holes goes to zero.

present is two well-demarcated regions in the black hole regime separated by a critical line, as described above.

V. DISCUSSION

We have presented evidence for the existence of a new type of critical phenomena within the black hole regime of the spherically symmetric Einstein-Yang-Mills model. Previous work on critical behavior in this model has established that both type I and type II critical solutions emerge in sufficiently general families of initial data. However, that earlier work was unable to accurately evolve to the future of black hole formation. Using a different coordinate system and horizon excision techniques, we are able to evolve well into the black hole regime. We find that these two different types of critical collapse can be generalized to types of collapsing spacetimes with a distinguishing characteristic being the asymptotic vacuum value of the Yang-Mills potential. These two ''phases'' of black hole formation are separated by a critical line in phase space such that dynamically forming black hole solutions exactly at criticality are the static, $n=1$ colored black holes [13,14]. This, of course, fits nicely within our conceptual framework that critical solutions are intermediate attractors of co-dimension one.

It is worth emphasizing a few observations at this point. First, it is important to note that the mass of the final Schwarzschild black hole in the evolution will be discontinuous across this new critical line in Fig. 4. (In fact, indications of jumps in the black hole mass-spectrum in the supercritical regime were present in earlier calculations [21].) Naively, this might be somewhat surprising since it means that nearby configurations in the space of initial data can have, in principle, very different sized black holes as their end-states.

Further, we note that when the colored black holes were originally investigated, it was found that the nth static colored black hole is parametrized by its horizon radius, r_h. In addition, as $r_h\rightarrow0$, the black hole solution approaches the corresponding nth Bartnik-Mckinnon solution. In the dynamical context discussed here for the $n=1$ solutions, one notices an interesting manifestation of this result. The colored black hole attractors separating the type I and type II regions in Fig. 4, are likewise parametrized by their horizon radius in such a way that as the ''triple point'' is approached, $r_h\rightarrow0$, and the Bartnik-Mckinnon solution emerges as the relevant attractor separating type I collapse from dispersion.

Finally, it is natural to ask if other collapsing systems might exhibit similar behavior. Indeed, one can simply look in the literature on static, hairy black holes and point to a number of systems that one would conjecture should have a ''phase diagram'' similar to Fig. 4. Such theories should include Einstein-Yang-Mills coupled to a dilaton (EYMD) and the Einstein-Skyrme system. However, there are other examples of systems which exhibit both type I and type II

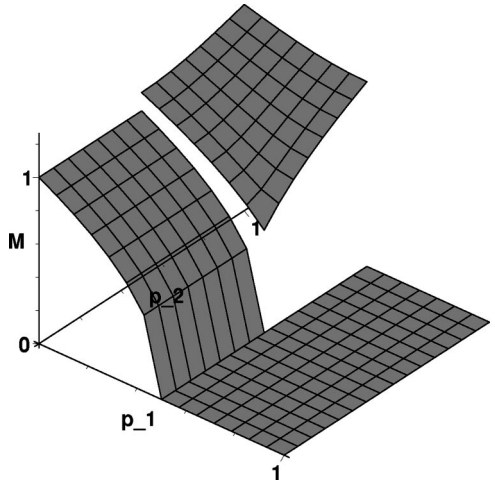

FIG. 5. This is a *schematic* plot of the final black hole mass as a function of the two initial data parameters. One should compare this plot with Fig. 4. If one imagines looking at a 3 dimensional version of that figure viewed from the upper right hand corner, the result should be something like this. The zero (flat) portion of the graph corresponds to dispersion of the collapsing fields. Exactly type II critical solutions sit along the left side of the critical line with the masses of super-critical black holes forming a continuous transition from it. Exactly type I critical solutions (which are not black holes) sit on the right side of the critical line which marks the discontinuity in the black hole masses of super-critical black holes. Finally, the new transition is also a discontinuous one with the colored black holes sitting on the threshold between black holes formed via generalized type I and type II collapse.

critical behavior. These include a massive scalar field and (it is conjectured) a massive, charged scalar field [6]. These latter systems are particularly intriguing in light of the results presented here because though they do exhibit type I and type II critical behavior, no-hair theorems suggest that these systems will not have static black hole solutions other than Kerr (or Schwarzschild, in spherical symmetry). It should thus be of interest to investigate the nature of the super-critical regime for these, and possibly other, systems.

ACKNOWLEDGMENTS

This research has been supported in part by NSF grants PHY93-18152, PHY94-07194 and PHY97-22068. M.W.C. would like to thank P. Bizon and T. Chmaj for useful communications [21], including descriptions of unpublished results which indicated that the parameter-space regime studied here might lead to colored black holes.

APPENDIX

We collect here some of the details involved in deriving the equations of motion used in the paper, and to present a somewhat more general framework for future work on the Einstein-Yang-Mills system (EYM). The action for our model is

$$S=\int d^4x\sqrt{-g}\left[\frac{R}{16\pi G}-\frac{1}{g^2}F^a_{\mu\nu}F^{a\mu\nu}\right] \tag{A1}$$

where $F^a_{\mu\nu}$ is the Yang-Mills field strength tensor. As usual, Greek indices range over the four spacetime dimensions and Latin indices indicate group indices. Spacetime indices are raised and lowered by the metric $g_{\mu\nu}$ while we will not lower group indices. Thus, repeated upper group (Latin) indices will be summed over.

The equations of motion are found by varying the action with respect to the fields. Varying with respect to the metric yields the Einstein equations

$$\frac{1}{16\pi G}G_{\mu\nu}=T_{\mu\nu}=\frac{1}{g^2}\left(2F^a_{\mu\lambda}F^{a\lambda}_{\nu}-\frac{1}{2}g_{\mu\nu}F^a_{\alpha\beta}F^{a\alpha\beta}\right). \tag{A2}$$

Varying with respect to the connection A^a_μ gives

$$D_\mu F^{a\mu\nu}=\nabla_\mu F^{a\mu\nu}+\epsilon^{abc}A^b_\mu F^{c\mu\nu}=0. \tag{A3}$$

With the general equations in hand we are in a position to make some simplifying assumptions. To begin, we assume that we have an $SU(2)$ gauge field. In addition we will assume spherical symmetry. The most general parametrization of the spacetime metric is then

$$ds^2=(-\alpha^2+a^2\beta^2)dt^2+2a^2\beta dtdr+a^2dr^2+b^2r^2d\Omega^2 \tag{A4}$$

where the metric coefficients α, β, a and b will depend on the temporal and radial coordinates t and r and $d\Omega^2$ is the usual metric on the unit two-sphere. Likewise, the most general parametrization of the gauge connection is now

$$A=u\,\tau^r dt+v\,\tau^r dr+(w\,\tau^\theta+\tilde{w}\,\tau^\phi)d\theta$$
$$+(\cot\theta\,\tau^r+w\,\tau^\phi-\tilde{w}\,\tau^\theta)\sin\theta d\phi.$$

where the coefficients u, v, w and $\tilde{w}$ will all depend on t and r. The τ^a are the spherical projection of the Pauli spin matrices and form an anti-Hermitian basis for the group $SU(2)$ satisfying $[\tau^a,\tau^b]=\epsilon^{abc}\tau^c$ with $a,b,c\in\{r,\theta,\phi\}$. We note that this connection is invariant under a gauge transformation of the form $U=e^{\psi(t,r)\tau^r}$. The field strength derived from this connection is

$$F=\tau^r(\dot{v}-u')dt\wedge dr+[(\dot{w}-u\tilde{w})dt+(w'-v\tilde{w})dr]$$
$$\wedge(\tau^\theta d\theta+\tau^\phi\sin\theta d\phi)+[(\dot{\tilde{w}}+uw)dt+(\tilde{w}'+vw)dr]$$
$$\wedge(\tau^\phi d\theta-\tau^\theta\sin\theta d\phi)-(1-w^2-\tilde{w}^2)\tau^r d\theta\wedge\sin\theta d\phi. \tag{A5}$$

With these assumptions, the equations of motion for the Yang-Mills fields can now be written in first order (in time) form as

$$\dot{\Pi}=\left[\beta\Pi+\frac{\alpha}{a}\Phi\right]'+uP-v\left(\beta P+\frac{\alpha}{a}Q\right)$$
$$+\frac{\alpha a}{b^2r^2}w(1-w^2-\tilde{w}^2) \tag{A6}$$

$$\dot{P}=\left[\beta P+\frac{\alpha}{a}Q\right]'-u\Pi+v\left(\beta\Pi+\frac{\alpha}{a}\Phi\right)+\frac{\alpha a}{b^2r^2}\tilde{w}(1-w^2-\tilde{w}^2) \tag{A7}$$

$$Y'=\tilde{w}\Pi-wP \tag{A8}$$

$$\dot{Y}=\frac{\alpha}{a}(\tilde{w}\Phi-wQ)+\beta(\tilde{w}\Pi-wP) \tag{A9}$$

where we have used the definitions

$$\Pi=\frac{a}{\alpha}[\dot{w}-u\tilde{w}-\beta(w'-v\tilde{w})] \tag{A10}$$

$$\Phi=w'-v\tilde{w} \tag{A11}$$

$$P=\frac{a}{\alpha}[\dot{\tilde{w}}+uw-\beta(\tilde{w}'+vw)] \tag{A12}$$

$$Q=\tilde{w}'+vw \tag{A13}$$

$$Y=\frac{b^2r^2}{2\alpha a}(\dot{v}-u'). \tag{A14}$$

We also have evolution equations for Φ and Q:

$$\dot{\Phi}=\left[\frac{\alpha}{a}\Pi+\beta\Phi\right]'+uQ-v\left[\frac{\alpha}{a}P+\beta Q\right]-\tilde{w}\frac{2\alpha a}{b^2r^2}Y \tag{A15}$$

$$\dot{Q}=\left[\frac{\alpha}{a}P+\beta Q\right]'-u\Phi+v\left[\frac{\alpha}{a}\Pi+\beta\Phi\right]+w\frac{2\alpha a}{b^2r^2}Y, \tag{A16}$$

which follow from differentiation of (A11) and (A13) with respect to time, and elimination of explicit time derivatives using the definitions (A10)–(A14).

Finally, the relevant Einstein equations are the evolution equations for the metric components and the components of the extrinsic curvature, together with the Hamiltonian and momentum constraints, as follows:

$$\dot{a}=-a\alpha K^r{}_r+(a\beta)' \tag{A17}$$

$$\dot{b}=-\alpha bK^\theta{}_\theta+\frac{\beta}{r}(rb)' \tag{A18}$$

$$\dot{K}^r{}_r=\beta K^r{}_r{}'+\alpha K^r{}_rK-\frac{1}{a}\left(\frac{\alpha'}{a}\right)'-\frac{2\alpha}{arb}\left[\frac{(rb)'}{a}\right]'+4\pi G\alpha[S-\rho-2S^r{}_r] \tag{A19}$$

$$\dot{K}^\theta{}_\theta=\beta K^{\theta\prime}_\theta+\alpha K^\theta{}_\theta K+\frac{\alpha}{(rb)^2}-\frac{1}{a(rb)^2}\left(\frac{\alpha rb}{a}(rb)'\right)'+4\pi G\alpha[S-\rho-2S^\theta{}_\theta] \tag{A20}$$

$$-\frac{2}{arb}\left\{\left(\frac{(rb)'}{a}\right)'+\frac{1}{rb}\left[\left(\frac{rb}{a}(rb)'\right)'-a\right]\right\}+4K^r{}_rK^\theta{}_\theta+2K^{\theta2}_\theta=16\pi G\rho \tag{A21}$$

$$-\frac{(rb)'}{rb}(K^\theta{}_\theta-K^r{}_r)-K^{\theta\prime}_\theta=4\pi Gj_r. \tag{A22}$$

Here, ρ is the energy density, j_r is the momentum density and $S^r{}_r$, $S^\theta{}_\theta$ and $S^\phi{}_\phi$ are the stress energy components projected onto our spacelike hypersurface. Explicitly, we have

$$\rho=\frac{1}{4g^2}\left\{\frac{4Y^2}{b^4r^4}+\frac{(1-w^2-\tilde{w}^2)^2}{b^4r^4}+\frac{2}{b^2r^2a^2}[Q^2+\Phi^2+P^2+\Pi^2]\right\} \tag{A23}$$

$$S^r{}_r=\frac{1}{4g^2}\left\{-\frac{4Y^2}{b^4r^4}-\frac{(1-w^2-\tilde{w}^2)^2}{b^4r^4}+\frac{2}{b^2r^2a^2}[Q^2+\Phi^2+P^2+\Pi^2]\right\} \tag{A24}$$

$$S^\theta{}_\theta=\frac{1}{4g^2}\left\{\frac{4Y^2}{b^4r^4}+\frac{(1-w^2-\tilde{w}^2)^2}{b^4r^4}\right\} \tag{A25}$$

$$S^\phi{}_\phi=S^\theta{}_\theta \tag{A26}$$

$$j_r=-\frac{1}{g^2ab^2r^2}(\Pi\Phi+PQ). \tag{A27}$$

As can be seen, we have chosen to write things in a fairly general form. Indeed, this is the most general EYM theory we could consider in spherical symmetry. We can thus consider more general matter configurations, together with a greater variety of coordinate systems than have been considered to date. Subsets of these equations have been investigated before in different contexts. For example, static versions of these equations have been studied in order to understand particle-like solutions and colored black holes. In addition, [5] evolved a version of these equations in polar ($K^\theta{}_\theta=0$), areal ($b=1$) coordinates with the additional assumption on the Yang-Mills field that the connection $A_\mu{}^a$ was purely magnetic.

For our work here, we will also make this ''magnetic *ansatz*.'' More specifically, we will assume that the electric charge density, Y, is identically zero. In addition to this *ansatz*, we also make the following gauge choice: $v=0$. Making this gauge choice leaves the connection invariant under a gauge transformation of the form $U=e^{\psi(t)\tau^r}$. From the definition for Y in Eq. (A14) we see that the function u, by these assumptions, depends only on t. However, the residual gauge freedom implies that u is arbitrary up to a function of t. We can thus fix the remaining gauge freedom in the following way. Choosing $u=0$ fixes the gauge up to a constant gauge

transformation of the form $U=e^{\psi r^r}$ where ψ is now a constant. This has the effect of sending w and $\tilde{w}$ into linear combinations of each other. such that choosing a value for ψ (such as zero) picks out a particular combination of these remaining connection coefficients. Thus, without loss of generality, we can choose $\tilde{w}=0$ and we see that in the context of this particular problem, the magnetic *ansatz* has effectively set all the fields but w to zero.

As discussed in the body of the paper, we want to be able to evolve the system for long times to the future of any black hole formation. To this end, we choose a coordinate system with maximal slicing: $K=K^r{}_r+K^\theta{}_\theta+K^\phi{}_\phi=0$. We will retain the choice of areal, or radial, coordinates ($b=1$) so that the coordinate r is immediately related to the area of origin-centered two-spheres.

Given all these assumptions, the equations which we must solve simplify considerably. The evolution equations are

$$\dot{\Pi}=\left[\beta\Pi+\frac{\alpha}{a}\Phi\right]'+\frac{\alpha a}{r^2}w(1-w^2) \tag{A28}$$

$$\dot{\Phi}=\left[\frac{\alpha}{a}\Pi+\beta\Phi\right]' \tag{A29}$$

$$\dot{w}=\frac{\alpha}{a}\Pi+\beta w' \tag{A30}$$

and the constraint equations are

$$w'=\Phi \tag{A31}$$

$$\alpha''=\alpha'\left(\frac{a'}{a}-\frac{2}{r}\right)+\frac{2\alpha}{r^2}\left(a^2-1+\frac{2ra'}{a}\right)+4\pi G\alpha(S-3\rho) \tag{A32}$$

$$a'=a\frac{1-a^2}{2r}+\frac{3}{2}ra^3K_\theta{}^{\theta 2}+4\pi Gra\rho \tag{A33}$$

$$K_\theta{}^{\theta\prime}=-\frac{3}{r}K_\theta{}^\theta+4\pi G\left(\frac{\Pi\Phi}{g^2ar^2}\right) \tag{A34}$$

where the matter stress-energy terms are given by

$$S-3\rho=\frac{a^2(1-w^2)^2}{2g^2r^4}+\frac{1}{g^2r^2}(\Phi^2+\Pi^2) \tag{A35}$$

$$\rho=\frac{a^2(1-w^2)^2}{4g^2r^4}+\frac{1}{2g^2r^2}(\Phi^2+\Pi^2). \tag{A36}$$

Finally, we have an algebraic condition for the non-vanishing component of the shift vector

$$\beta=\alpha rK_\theta{}^\theta, \tag{A37}$$

which follows from (A18) with $b(r,t)\equiv 1$.

[1] M.W. Choptuik, Phys. Rev. Lett. **70**, 9 (1993).
[2] A.M. Abrahams and C.R. Evans, Phys. Rev. Lett. **70**, 2980 (1993).
[3] C.R. Evans and J.S. Coleman, Phys. Rev. Lett. **72**, 1782 (1994).
[4] C. Gundlach, Adv. Theor. Math. Phys. **2**, 1 (1998).
[5] M.W. Choptuik, P. Bizon, and T. Chmaj, Phys. Rev. Lett. **77**, 424 (1996).
[6] P.R. Brady, C.M. Chambers, and S.M.C.V. Goncalves, Phys. Rev. D **56**, 6057 (1997).
[7] P. Bizon and T. Chmaj, Phys. Rev. D **58**, 041501 (1998).
[8] P. Bizon and T. Chmaj, Acta Phys. Pol. B **29**, 1071 (1998).
[9] P. Bizon, T. Chmaj, and Z. Tabor, Phys. Rev. D **59**, 104003 (1999).
[10] R. Bartnik and J. Mckinnon, Phys. Rev. Lett. **61**, 141 (1988).
[11] E. Seidel and W-M. Suen, Phys. Rev. Lett. **66**, 1659 (1991).
[12] P. Bizon and T. Chmaj, Phys. Lett. B **297**, 55 (1992).
[13] P. Bizon, Phys. Rev. Lett. **64**, 2844 (1990).
[14] M.S. Volkov and D.V. Gal'tsov, Pis'ma Zh. Éksp. Teor. Fiz. **50**, 312 (1990) [JETP Lett. **50**, 346 (1990)].
[15] E. Seidel and W-M. Suen, Phys. Rev. Lett. **69**, 1845 (1992).
[16] R.L. Marsa and M.W. Choptuik, Phys. Rev. D **54**, 4929 (1996).
[17] R.L. Marsa and M.W. Choptuik, ''The RNPL User's Guide,'' http://wwwrel.ph.utexas.edu/Members/marsa/rnpl/users_guide/users_guide.html (1995).
[18] N. Straumann and Z. H. Zhou, Phys. Lett. B **243**, 33 (1990).
[19] Z.H. Zhou, Helv. Phys. Acta **65**, 767 (1992).
[20] M.S. Volkov, O. Brodbeck, G. Lavrelashvili, and N. Straumann, Phys. Lett. B **349**, 438 (1995).
[21] P. Bizon and T. Chmaj (private communication).